bound is 2.02 for $k = \frac{1}{4}$, and 2.17 for $k = \frac{1}{2}$. However, for the range of γ under construction and for the given transient input, the total stress $\sigma_{\theta\theta} = \sigma_{\theta\theta_0} + \sigma_{\theta\theta_2}$ at no time exceeds its instantaneous steady-state value.

The curves for $k = \frac{3}{4}$ in Figs. 5 and 6 also give an indication of the error involved in neglecting transient effects and assuming instantaneous steady-state conditions for relatively thick "thin sections."

Simple expressions may be obtained for the maximum compressive and tensile stresses in thin sections. Designating h as a dimensionless thickness, i.e.,

$$h = 1 - k \tag{60}$$

and maintaining terms to order h^2, the transient terms for a continuous $Q_0(t)$ are of order h^3 or greater and negligible. The maximum tensile stress at $\theta = 0$, $r = k$, as evaluated from the corresponding steady-state solution of (56) and (57), is then given by

$$\sigma_{\theta\theta}]_{\substack{r=k \\ \theta=0}} = \left(\frac{1+\nu}{1-\nu}\right)\frac{G'\alpha R_0 h Q_0(t)}{K}\left[1 + (\gamma + \tfrac{2}{3})h\right] \tag{61}$$

and the maximum compressive stress at $\theta = 0$, $r = 1$ is given by

$$\sigma_{\theta\theta}]_{\substack{r=1 \\ \theta=0}} = -\left(\frac{1+\nu}{1-\nu}\right)\frac{G\alpha R_0 h Q_0(t)}{K}\left[1 - (\tfrac{5}{3} - 2\gamma)h\right] \tag{62}$$

With $h = 0.1$ ($k = 0.9$), the error in (61) and (62) is less than 3.5% in the steady state for all γ.

As previously stated, the form of the heat input over the back surface of the sphere cannot be considered physically valid, and the preceding analysis is restricted to an area around the nose. The boundary conditions (47) and (48) present an insulated surface at the equatorial plane $z = 0$, whereas in actual fact some heat transfer can be expected to take place across this plane from the forward portion of the hollow sphere to the rear portion. Also, in applications to hemispherically capped cylinders and cones capped by a spherical segment, localized discontinuity stresses may be present at the junction of the cap and cylinder or cone. The preceding results, however, should be quite representative of the actual stresses in the aerodynamically heated thick-walled sphere or hemisphere in the region $0 \leq \theta \leq \pi/3$.

References

[1] Boley, B. A. and Weiner, J. H., *Theory of Thermal Stresses* (John Wiley and Sons Inc., New York, 1960), Chap. IX, p. 304.

[2] Parkus, H., *Instationäre Wärmespannungen* (Springer, Vienna, Austria, 1959), Chap. II, p. 64.

[3] Timoshenko, S. and Goodier, J. N., *Theory of Elasticity* (McGraw-Hill Book Co. Inc., New York, 1951), 2nd ed., Chap. XIV, pp. 416–421.

[4] Trostel, R., "Instationäre Wärmespannungen in einer Hohlkugel," Ingr.-Arch. **24**, 373–391 (1956).

[5] McDowell, E. L. and Sternberg, E., "Axisymmetric thermal stresses in a spherical shell of arbitrary thickness," J. Appl. Mech. **24**, 376–380 (1957).

[6] Melan, E., "Wärmespannungen bei der Abkuhlung einer Kugel," Acta. Phys. Austriaca **10**, 81–86 (1956).

[7] Carslaw, H. S. and Jaeger, J. C., *Conduction of Heat in Solids* (Clarendon Press, Oxford, 1959), 2nd ed., Chap. I, pp. 30–32.

[8] Sternberg, E., Eubanks, R. A., and Sadowsky, M. A., "On the axisymmetric problem of elasticity theory for a region bounded by two concentric spheres," Proc. First U. S. Natl. Congr. Appl. Mech., 209–215 (1952).

[9] Morse, P. M. and Feshbach, H., *Methods of Theoretical Physics* (McGraw-Hill Book Co. Inc., New York, 1953), Part II, p. 1573.

[10] Lees, L., "Laminar heat transfer over blunt-nosed bodies at hypersonic flight speeds," Jet Propulsion **26**, 259–269 (1956).

[11] Bloxsom, D. E. and Rhodes, B. V., "Experimental effect of bluntness and gas rarefaction on drag coefficients and stagnation heat transfer on axisymmetric shapes in hypersonic flow," J. Aerospace Sci. **29**, 1429–1432 (1962).

[12] Ferri, A. and Zakhay, V., "Measurements of stagnation point heat transfer at low Reynolds numbers," J. Aerospace Sci. **29**, 847–850 (1962).

NOVEMBER 1963 AIAA JOURNAL VOL. 1, NO. 11

Buckling of Cylindrical Shells under Dynamic Loads

J. D. Wood*

Mechanics Research, Inc., El Segundo, Calif.

AND

L. R. Koval†

Space Technology Laboratories Inc., Redondo Beach, Calif.

The results of an exploratory experimental and analytical program on the buckling (collapse) of thin-walled cylindrical shells under dynamic loads are presented and discussed. Loading conditions for the cylinders include dead-weight axial compression with axisymmetric transient and oscillatory hydrostatic pressures. Where possible, the experimental results are qualitatively verified by linear shell theory. Areas requiring further experimental and theoretical study are identified.

I. Introduction

In missile and space vehicle design there is an ever-increasing number of cases in which shell structures are subjected to dynamic loads. One common loading condition for cylindrical shells is a sustained axial compression with dynamic external lateral loads. Consequently, one might expect that a condition of structural instability resulting from lateral dynamic loading could exist for thin shells.

Presented at the AIAA Launch and Space Vehicle Shell Structures Conference, Palm Springs, Calif., April 1–3, 1963; revision received September 3, 1963. This work was supported by NASA Headquarters under Contract No. NASr-56. Appreciation is expressed to M. G. Rosche of NASA Headquarters and M. V. Barton, Director of the Engineering Mechanics Laboratory, Space Technology Laboratories Inc., for their encouragement, suggestions, and assistance throughout the program, and to J. P. O'Neill, R. F. Wells, and D. A. Evensen of Space Technology Laboratories for their direction and performance of the experiments.

* Vice President; formerly Associate Manager, Dynamics Department, Engineering Mechanics Laboratory, Space Technology Laboratories Inc., Redondo Beach, Calif.

† Member of the Technical Staff.

Recently, it has been recognized that random pressure fluctuations of considerable magnitude are generated around missile structures during transonic and low supersonic speeds, as shown by recent wind tunnel tests.‡ It has been shown that this phenomenon, called buffeting, was a critical loading condition on recent space probes and on the Mercury vehicle; however, because of the lack of data and knowledge, the existence of "dynamic buckling" (collapse§) for the shell structures in these cases was not considered. Other situations where shells are under large axial compression and lateral dynamic loads occur during missile silo launch and during nuclear attacks on re-entry vehicles outside of the atmosphere (x-ray ablation).

Although a number of studies of dynamic buckling have been made, a large portion of this work has been concerned with column and plate behavior. Cylinders have been treated to some extent chiefly by Russian investigators.[2–11] Problems of the stability under parametric resonance were discussed in Refs. 6, 12, 13, and 18. To the authors' knowledge, the present problem has not been discussed.

This paper presents some of the experimental and theoretical results of an exploratory program on the stability of cylindrical shells subject to dynamic loads. The primary purpose of the program was to investigate in a limited time the nature of buckling in thin-walled cylindrical shells that are subjected to sustained axial compression and rapidly varying normal pressures. Other details of the program, such as loading conditions of axisymmetric and asymmetric impulsive and asymmetric stepwise pressures, and the many facets of the experimental techniques and apparatus, are given in Ref. 1.

II. Test Specimens and Equipment

All test specimens used in this program are right circular cylinders with the following geometric characteristics: length (L) = 8 in., radius (R) = 4 in., and thickness (h) = 0.005 and 0.0075 in. The specimens were constructed of type A Dupont "Mylar" Polyester film. The details of their fabrication may be found in Ref. 1. Mylar is attractive for investigations of this kind because it can withstand large amounts of strain without excessive permanent set, thereby permitting repetitive tests of each specimen.

Several possible methods of producing rapid external pressure engulfment of a cylindrical specimen were considered, such as small explosive charges near the specimen, cylindrical sheets of explosive wrapped around the specimen, an array of quick-opening valves admitting pressurized air to a chamber around the specimen, or mounting the specimen inside a shock tube. All of these methods presented difficult pressure control problems or difficulty in observing the specimen under test. It was therefore decided to study means of evacuating the interior of the specimen.

The technique finally selected produces the pressure differential by means of an electromagnetically driven piston connected to the interior of the specimen (see Figs. 1 and 2 for photos and a schematic of the apparatus). Motion of the piston produces a negative pressure in the interior of the specimen, and, with atmospheric pressure acting on the exterior, a uniform inward force over the surface of the specimen is produced.

The driver is made from a loudspeaker magnet assembly, and the piston is a modified lightweight loudspeaker cone assembly incorporating a special edge support that allows an unusually long stroke for the cone piston.

‡ NASA, Ames Research Center, Moffett Field, Calif., wind tunnel tests on Advent and Atlas-Able-5 configurations; AEDC, 16 ft PWT tests on the Mercury vehicle.

§ Throughout this paper the word "buckling" is synonymous with "collapse." Unbounded response in such a dynamic response problem results in collapse.

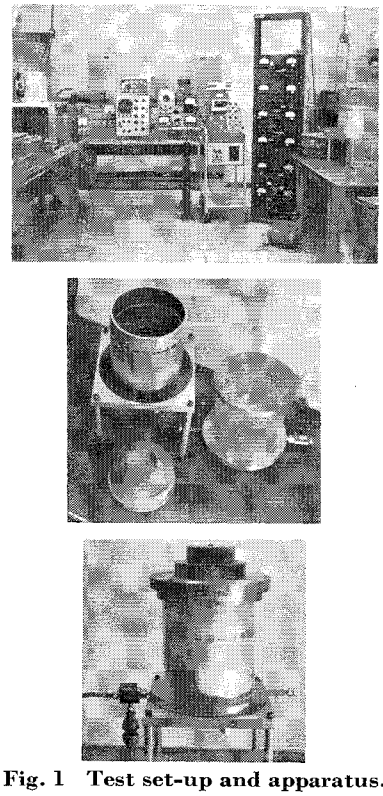

Fig. 1 Test set-up and apparatus.

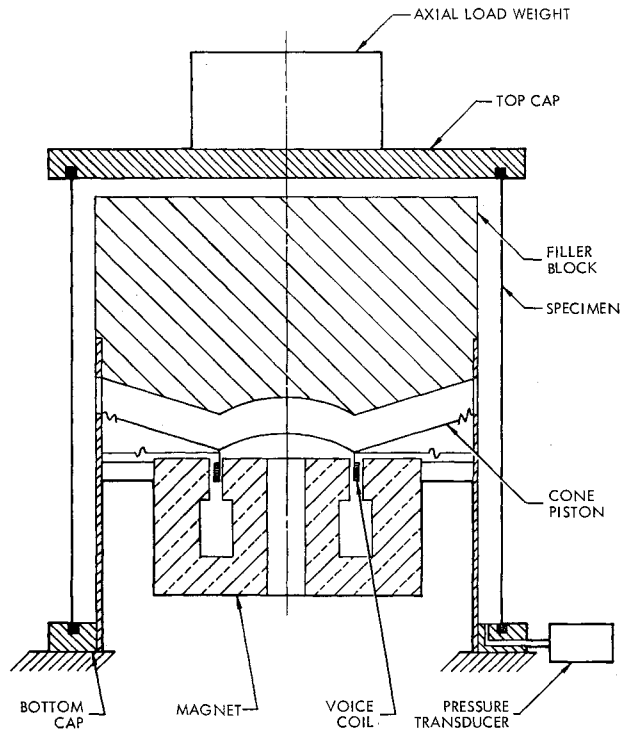

Fig. 2 Schematic of apparatus.

III. Loading Conditions and Results

A. Dead-Weight Axial Load and Stepwise Axisymmetric Hydrostatic Pressures

1. *Procedure*

In this test a clamped cylinder was loaded with dead weights at one end (see Figs. 1 and 2) and was then subjected to a stepwise axisymmetric hydrostatic pressure.

Considerable effort was expended in developing a technique for programming a pressure differential that was effectively a step function in time. By using the electromagnetically

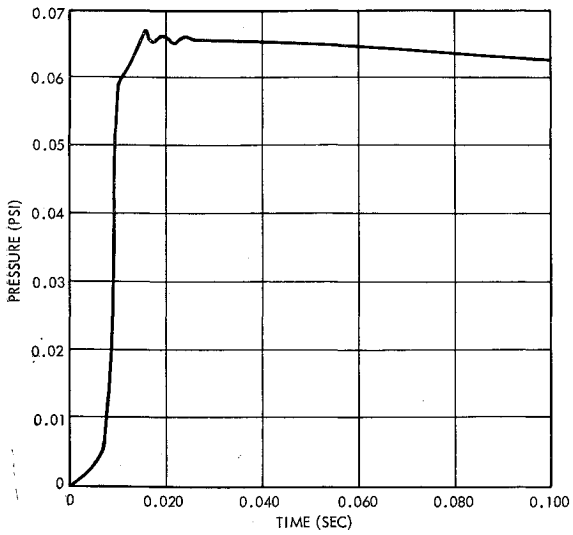

Fig. 3 Typical ramp-step pressure record.

driven piston described previously, the step function had the following characteristics: rise time, approximately 3 msec; overshoot, less than 5% of the total amplitude; duration of the pulse (defined as the time required for the amplitude of the pressure to drop 5%), 60 msec as compared to 8 msec, which is the usual collapse time. Figure 3 gives the details of a typical pressure record of the step function which was obtained with the apparatus shown in Figs. 1 and 2.

The following procedure was used to obtain a comparison of the specimen response due to static loads and stepwise dynamic loads. The desired axial load was applied by placing circular steel weights on the upper cap. A *slowly* increasing differential pressure was then applied to the specimen by means of a vacuum pump until collapse occurred. Collapse of the specimen, in the static and dynamic tests, was characterized by large buckle patterns and an inability to support axial load. After the specimen had been restored to the stable condition with zero pressure differential and the axial load was replaced, a series of pressure steps was applied. The amplitude of these steps was increased in increments until collapse of the specimen occurred. In this manner the maximum pulse that could be applied without collapsing the specimen was determined. This procedure was repeated for several values of axial load. The data from these tests are plotted in Figs. 4 and 5.

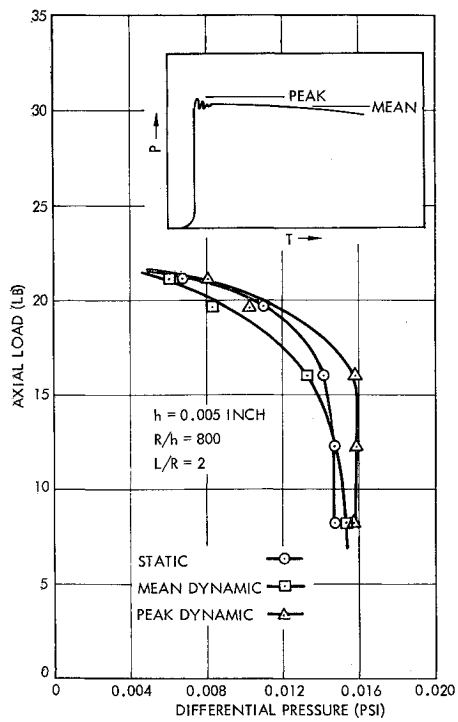

Fig. 4 Collapse load interaction curve for a Mylar cylinder under a ramp-step pressure; h = 0.005 in.

2. *Results*

The application of a stepwise axisymmetric hydrostatic pressure to the cylinder did not produce collapse at a value significantly different from that found when the pressure was applied statically. Since a rise time of approximately 3 msec seemed to be a minimum with the present apparatus and no degradation in the load-carrying ability of the shell was detected, longer rise times were not investigated.

The results of these tests are verified with linear shell theory, as discussed later. However, it is hypothesized that nonlinear theory, which can account for the interaction or exchange of energy between the extensional and inextensional modes, may show that the load-carrying ability of the shell as compared with static loading can be different if the pressure is applied rapidly enough to excite the extensional mode. In this study, the 3-msec rise time of the step is not short enough to excite the extensional mode (frequency of approximately 3000 cps) for the Mylar cylinder. In future studies, an attempt will be made to rectify this deficiency.

B. Dead-Weight Axial Load and Sinusoidal Axisymmetric Hydrostatic Pressures

1. *Procedure*

In most cases for this loading condition, the differential pressure on the cylinder fluctuated above and below atmospheric; however, it was also possible to apply a constant axisymmetric pressure by means of a vacuum pump and superimpose sinusoidal pressures. These pressures were measured by a transducer and recorded on an oscilloscope.

As before, the testing procedure consisted of two main parts: 1) static collapse tests, and 2) dynamic collapse tests. The first test of the cylinder determined the collapse load

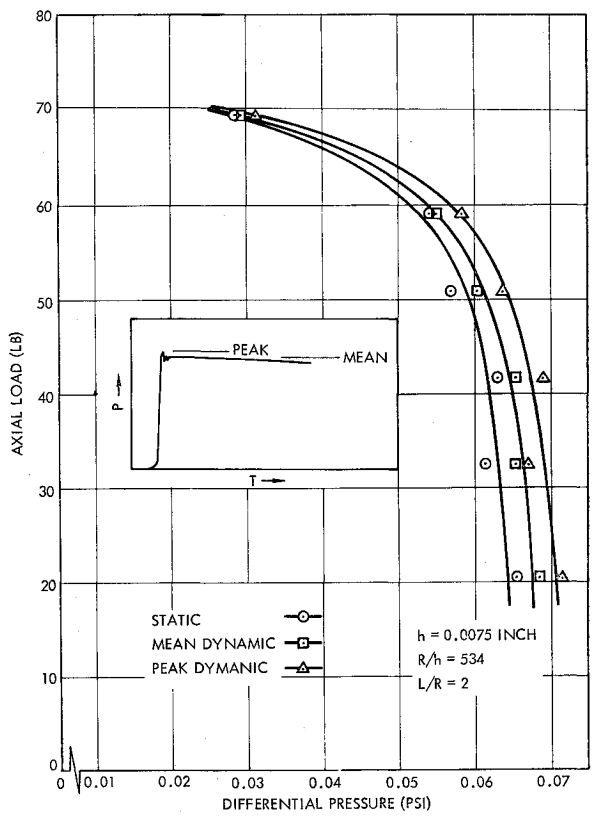

Fig. 5 Collapse load interaction curve for a Mylar cylinder under a ramp-step pressure, h = 0.0075 in.

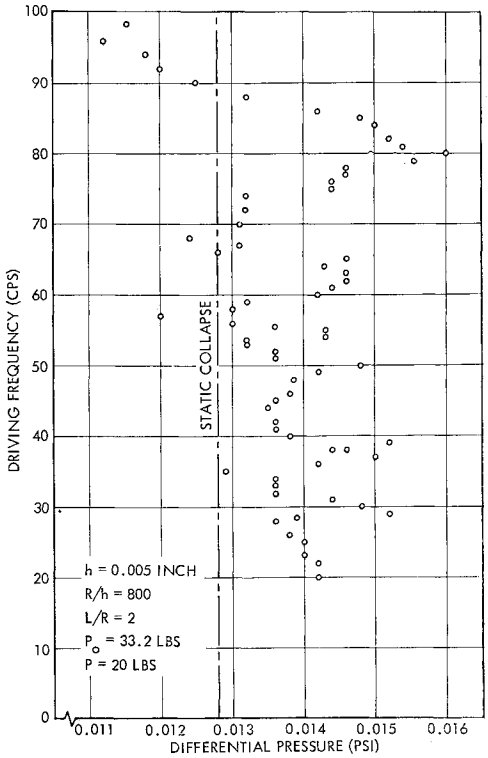

Fig. 6 Sinusoidal collapse pressure vs frequency for a Mylar cylinder; P_0 = 36.1 lb.

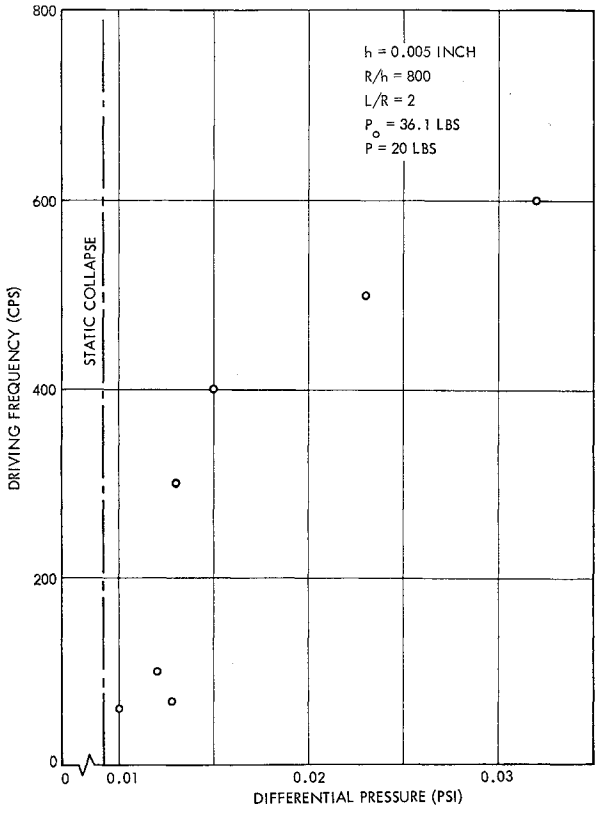

Fig. 7 Sinusoidal collapse pressure vs frequency for a Mylar cylinder; P_0 = 33.2 lb.

P_0 under static axial compression. Several runs with "rest" periods between each were made to determine this load accurately. Following this test, the static buckling pressure for an end load P was determined and used for comparison with the results of the dynamic tests (see Figs. 6 and 7).

Dynamic collapse tests were conducted by selecting a desired frequency and then increasing the amplitude of the pressure fluctuation until collapse occurred. The internal

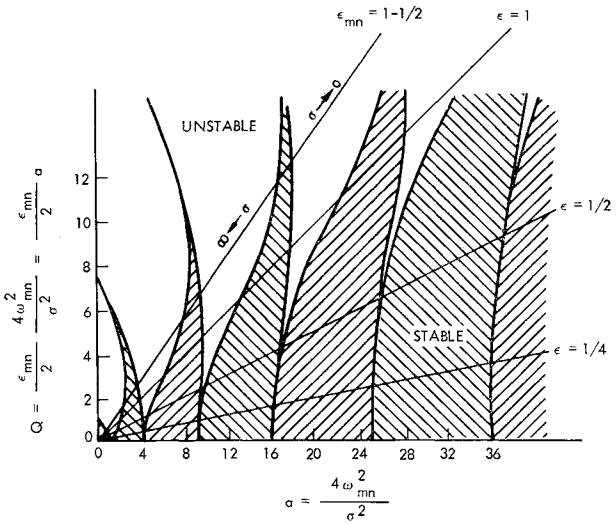

Fig. 8 Stability diagram for Mathieu's equation.

pressure oscillated above and below atmospheric pressure, and the half amplitude (maximum negative value) of the differential pressure across the shell when collapse occurred was recorded as the "dynamic collapse pressure." Care was taken to measure this amplitude when the internal pressure was below atmospheric, i.e., when the cylinder was subjected to a differential pressure tending to collapse rather than stabilize it.

2. *Results*

Two different cylinders were tested with the same R/h ratios but with different values of the collapse load P_0. One cylinder was tested in the frequency range 20 to 600 cps, and the second cylinder was tested in the frequency range 20 to 100 cps. The results of these tests are presented in Figs. 6 and 7.

The experimental results indicate that the pressure amplitude necessary to cause collapse can vary significantly with the driving frequency. For the cylinders tested, the pressure amplitude necessary to cause collapse varied from 90 to 350% of the static collapse pressure, depending upon the frequency.

As the driving frequencies increase, the collapse pressures also increase as shown in Fig. 7; such results agree with intuition. However, based on the variations found between 20 and 100 cps, it is felt that more data are needed to outline the results at the higher frequencies.

Using linear theory, as shown later, the response and stability of the shell are characterized by a Mathieu equation (see Fig. 8). Qualitatively, the predictions of this theory are borne out by the experiments.

Some experiments were conducted with a sinusoidal pressure acting simultaneously with a constant pressure. The latter is less than the static collapse pressure, and, in general, the results showed trends similar to those when the constant pressure is zero (see Fig. 9). However, Lubkin and Stoker[14] have shown for columns that it is possible to apply a constant load that is larger than the critical buckling value and still be stable, providing the total load (i.e., constant plus oscillatory) falls below the critical value during part of the cycle. Investigations such as this, for shells, are planned for the future.

IV. Analysis

A. Formulation of the Problem

A qualitative explanation for some of the experimental results can be obtained from an analysis employing linear shell theory. Since the stability phenomenon is essentially

one of buckling under axial load, attention is focused on the stability of the breathing modes into which the shell will buckle.

In the following, Donnell's theory[15] will be used so that the radial deformation is given by the solution to

$$k\nabla^8(w - w_1) + (1 - \nu^2)\frac{\partial^4(w - w_1)}{\partial x^4} - \nabla^4\left(\bar{N}_x\frac{\partial^2 w}{\partial x^2} + \bar{N}_\phi\frac{\partial^2 w}{\partial \phi^2} - \gamma\frac{\partial^2 w}{\partial t^2}\right) = 0 \quad (1)$$

where

w = radial component of total deformation, positive inward
w_1 = initial deformation from circular cross-section
x,ϕ = nondimensionalized coordinates
R = mean shell radius
ν = Poisson's ratio
$k = h^2/12R^2$, $\gamma = [\rho(1 - \nu^2)R^2]/E$
$\bar{N}_x = [N_x{}^0(1 - \nu^2)]/Eh$, $\bar{N}_\phi = [N_\phi{}^0(1 - \nu^2)]/Eh$

in which

$\nabla^4 = [(\partial^2/\partial x^2) + (\partial^2/\partial\phi^2)]^2$
$\nabla^8 = \nabla^4(\nabla^4)$
h = shell thickness
ρ = density
E = Young's modulus
$N_x{}^0, N_\phi{}^0$ = initial shell stress resultants

Equation (1) has been nondimensionalized with respect to the shell radius, and the initially deformed state has been treated in the manner of Timoshenko.[16] For the sake of simplicity, only radial inertia has been included, this being the principle inertial response.

For a shell subjected to a constant axial load P and an external hydrostatic pressure $q(t)$, the initial membrane loads can be computed by assuming the cylinder to remain circular and undergo a uniform compression circumferentially so that

$$N_x{}^0 = -(P/2\pi R) - \tfrac{1}{2}Rq(t), \qquad N_\phi{}^0 = -Rq(t) \quad (2)$$

For simplicity, the shell is assumed freely supported, and a solution is sought in the form

$$w(x,\phi,t) = \sum_{n=1}^{\infty}\sum_{m=1}^{\infty} f_{mn}(t)\sin\beta_m x\cos n\phi \quad (3)$$

where $f_{mn}(t)$ is the generalized coordinate of the m,nth mode, $\beta_m = m\pi/l$, $l = L/R$, and L = shell length. In the same spirit, the initially deformed state is described by

$$w_0(x,\phi) = \sum_{n=1}^{\infty}\sum_{m=1}^{\infty} f_{mn}'\sin\beta_m x\cos n\phi \quad (4)$$

Substituting Eqs. (2–4) into (1) and simplifying, one obtains for the generalized coordinate the equation

$$\frac{d^2 f_{mn}}{dt^2} + \frac{\beta_m{}^2}{\rho hR}\left[\frac{P_{mn_{cr}} - P}{2\pi R^2} - \left(\frac{1}{2} + \frac{n^2}{\beta_m{}^2}\right)q(t)\right]f_{mn} = \frac{\beta_m{}^2 P_{mn_{cr}} f_{mn}'}{2\pi\rho hR^3} \quad (5)$$

where

$$P_{mn_{cr}} = \frac{2\pi RhE}{\beta_m{}^2}\left[\frac{k(\beta_m{}^2 + n^2)^2}{1 - \nu^2} + \frac{\beta_m{}^4}{(\beta_m{}^2 + n^2)^2}\right]$$

is the critical axial buckling load for the m, nth mode in the absence of external pressure. The solution to the dynamic stability problem is thus reduced to the solution of (5) for a given pressure $q(t)$. Except where noted, instability is assumed synonomous with an unbounded displacement.

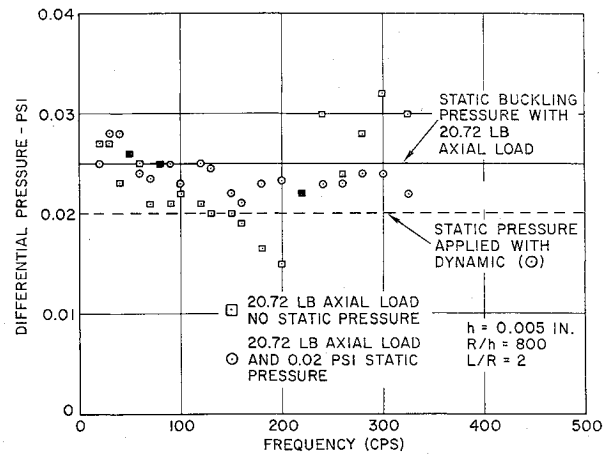

Fig. 9 Collapse pressure vs frequency for sinusoidal and constant pressure applied to a Mylar cylinder.

B. Ramp and Step Pressures

We consider in detail the case of a very rapidly applied pressure and mathematically represent it by

$$q(t) = q_1 H(t) \quad (6)$$

where $H(t)$ is the Heaviside unit step function. Substituting (6) into (5),

$$(d^2 f_{mn}/dt^2) + [A - BH(t)]f_{mn} = Cf_{mn}' \quad (7)$$

where

$$A = \frac{\beta_m{}^2}{\rho hR}\left(\frac{P_{mn_{cr}} - P}{2\pi R^2}\right)$$

$$B = \frac{\beta_m{}^2}{\rho hR}\left(\frac{1}{2} + \frac{n^2}{\beta_m{}^2}\right)q_1$$

$$C = \frac{\beta_m{}^2 P_{mn_{cr}}}{2\pi\rho hR^3}$$

$$f_{mn}(0) = f_{mn}'$$

Equation (7) is easily solved using Laplace transforms. The transform of (7) is

$$F(s) = \frac{f_{mn}'}{[s^2 + (A - B)]} + \frac{Cf_{mn}'}{s[s^2 + (A - B)]} \quad (8)$$

where s is the transform variable. The required solution is obtained by inverting (8), for which three cases exist.

1. *Subcritical pressure, $B < A$*

For this case, the inverse of (11) is

$$f_{mn}(t) = (f_{mn}'/\omega_{mn}{}^2)[\sin\omega_{mn}t + C(1 - \cos\omega_{mn}t)] \quad (9)$$

where

$$\omega_{mn}{}^2 = A - B = \frac{E}{\rho R^2}\left[k\frac{(\beta_m{}^2 + n^2)^2}{1 - \nu^2} + \frac{\beta_m{}^4}{(\beta_m{}^2 + n^2)^2} - \frac{\beta_m{}^2 P}{2\pi R^2} - \left(\frac{\beta_m{}^2}{2} + n^2\right)q_1\right]$$

The resulting motion is a pure oscillation about the initially deformed state at the modal natural frequency. There is no evidence of instability.

2. *Critical pressure, $B = A$*

In this case, the pressure is given by

$$q_1 = q_{mn_{cr}} = \frac{1}{[\frac{1}{2} + (n^2/\beta_m{}^2)]}\left(\frac{P_{mn_{cr}} - P}{2\pi R^2}\right) \quad (10)$$

and is the value required to induce buckling under static conditions. The solution is

$$f_{mn}(t) = f_{mn}'(t + \tfrac{1}{2}Ct^2) \tag{11}$$

and is clearly unbounded, with deflection increasing parabolically with time.

3. *Supercritical pressure, B > A*

Letting

$$\alpha^2 = B - A = \frac{\beta_m{}^2}{\rho h R}\left[\left(\frac{1}{2} + \frac{n^2}{\beta_m{}^2}\right) q_1 - \frac{P_{mn_{cr}} - P}{2\pi R^2}\right]$$

then

$$f_{mn}(t) = \frac{f_{mn}'}{\alpha^2}\,[\sinh\alpha t + C(1 - \cosh\alpha t)] \tag{12}$$

It is clear that the cylinder will buckle, since the response is unbounded.

4. *Comments and discussion*

Linear theory predicts no decrease in the critical pressure, even when it is quite suddenly applied. This result is primarily due to the "quasi-static" nature of Eq. (2). The primary response to the dynamic pressure is a "ring mode" in which the radial deformation can be assumed to be uniform and vary only with time. A corresponding free-body diagram of a shell element is shown in Fig. 10. The radial equation of motion is

$$N_\phi{}^0 = \rho h R(d^2w_0/dt^2) + Rq(t) \tag{13}$$

The stress-strain and strain-displacement relations yield

$$N_\phi{}^0 = \sigma_\phi{}^0 h = -Eh(w_0/R) \tag{14}$$

Upon eliminating w_0 between (13) and (14), the result is

$$\frac{d^2N_\phi{}^0}{dt^2} + \frac{E}{\rho R^2}N_\phi{}^0 = \frac{-E}{\rho R}\,q(t) \tag{15}$$

For the ramp pressure given by (see Fig. 11)

$$q(t) = (q_1/t_1)[tH(t) - (t - t_1)H(t - t_1)]$$

we obtain

$$N_\phi{}^0 = -q_1R\left(\frac{t}{t_1} - \frac{\sin\omega_R t}{\omega_R t_1}\right) \qquad 0 < t < t_1 \tag{16}$$

$$= -q_1R[1 + \eta\cos(\omega_R t + \phi)] \qquad t >$$

where

$$\eta = \frac{\sin(\pi t_1/T_R)}{(\pi t_1/T_R)}$$

$$T_R = 2\pi/\omega_R \qquad \omega_R = (1/R)[E/\rho]^{1/2}$$

In the limit $t_1 \to 0$, $\eta \to 1$, and the hoop stress corresponding to a step pressure becomes

$$N_\phi{}^0 = -q_1R(1 - \cos\omega_R t) \tag{16a}$$

which is the case previously considered.

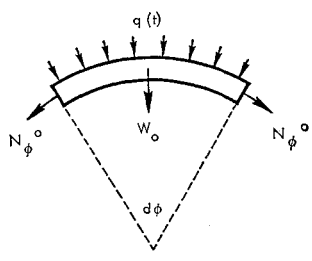

Fig. 10 Differential element of shell for ring mode.

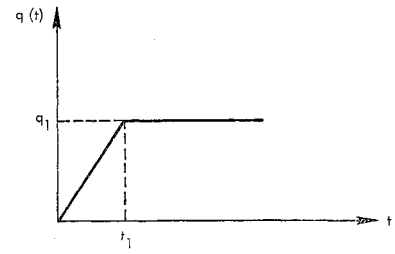

Fig. 11 Pressure-time history.

Equations (16) and (16a) indicate that for a rise time $t_1 \gg T_R$, where T_R is the natural period of the ring mode, $N_\phi{}^0$ is essentially its quasi-static value given by (2). The computation of $N_\phi{}^0$ by (2) thus implies a large rise time, and it is therefore not surprising that the preceding theory does not predict a degradation in critical pressure. However, (16) implies that a very short rise time can produce a maximum $N_\phi{}^0$ that is larger than its quasi-static value given by (2). A degradation in critical pressure may thus be possible if the rise time is short enough.

Equation (16) also explains the possible failure to detect degradation in the experimental work. For the Mylar test cylinders,

$$\omega_R = (1/R)[E/\rho]^{1/2} \approx 3000 \text{ cps}$$

so that $T_R = \frac{1}{3}$ msec, but the fastest rise time obtainable experimentally was $t_1 = 3$ msec.

For a better understanding of the coupling between the extensional and the breathing modes, a nonlinear analysis is required. Such a study has already been started, and preliminary results indicate that the critical pressure can be less if the rise time is short enough to excite the ring mode. Upon completion of this study, a detailed accounting of the results will be given in a later paper.

C. *Sinusoidal Pressure*

When $q(t)$ is given by

$$q(t) = q_0 + q_1\cos\sigma t \tag{17}$$

then the solution to (18) becomes

$$N_\phi{}^0 = -Rq_0 - \frac{Rq_1}{(\rho R^2/E)[(E/\rho R^2) - \sigma^2]}\cos\sigma t \tag{18}$$

If $\sigma \ll 1/R[E/\rho]^{1/2} = \omega_R$, then Eq. (18) becomes

$$N_\phi{}^0 \cong -R(q_0 + q_1\cos\sigma t) \tag{19}$$

For the Mylar test cylinders, $\omega_R = 3000$ cps, and this condition was certainly satisfied in the tests.

In addition to the axisymmetric radial motion, breathing modes are excited. Using (19) for (2) and then substituting into (5) and simplifying yields (initial imperfections are assumed negligible)

$$(d^2f_{mn}/dt^2) + \omega_{mn}{}^2(1 - \epsilon_{mn}\cos\sigma t)f_{mn} = 0 \tag{20}$$

where

$$\epsilon_{mn} = \frac{[\frac{1}{2} + (n^2/\beta_m{}^2)]q_1}{[(P_{mn_{cr}} - P)/2\pi R^2] - [\frac{1}{2} + (n^2/\beta_m{}^2)]}\,q_0$$

is a "load factor" giving the ratio of the amplitude of the sinusoidal component of pressure to the corresponding amount that can be applied statically. A load factor of $\epsilon_{mn} = 1$ corresponds to a cylinder that would be critically loaded under static conditions. Questions of considerable technical interest are: 1) Can the cylinder response be unstable when $\epsilon_{mn} < 1$? 2) Can the cylinder response be stable when $\epsilon_{mn} > 1$? The answer lies in the equation

$$(d^2f_{mn}/d\tau^2) + (a - 2Q\cos 2\tau)f = 0 \tag{21}$$

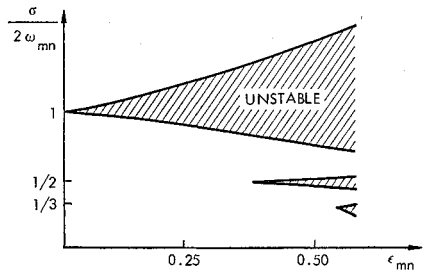

Fig. 12 Stability regions with damping present.

which is the standard form of Mathieu's equation[17] for which

$$\tau = \sigma t/2 \qquad a = 4\omega_{mn}^2/\sigma^2$$

$$Q = (\epsilon_{mn}/2)(4\omega_{mn}^2/\sigma^2)$$

Figure 8 shows the usual stability diagram associated with Eq. (21) showing the values of (a,Q) for which motion is stable or unstable. "Load lines" are drawn to facilitate the location of various loading conditions. From Fig. 8, the following conclusions can be drawn:

1) For $\epsilon_{mn} < 1$, the motion is essentially stable, but some unstable regions are present indicating that, for proper combinations of q_1 and σ, a subcritical sinusoidal pressure can induce "premature" buckling.

2) For $\epsilon_{mn} > 1$, the motion is generally unstable, but there are stable regions in which a supercritical q_1 can be applied without inducing buckling. This has been observed experimentally.

3) For σ high enough, the motion is always stable regardless of ϵ_{mn}. This agrees with intuition, for it represents the condition in which the pressure is applied and removed too rapidly for the shell to respond.

These predictions were qualitatively verified experimentally.

When Q is small, simple equations for the boundaries between stable and unstable regions can be written and critical frequencies determined for a given load factor ϵ_{mn}. The regions of instability have been determined to be

$$\frac{2\omega_{mn}}{[1 + (\epsilon/2) + (7/32)\epsilon^2 + (39/512)\epsilon^3]^{1/2}} < \sigma < \frac{2\omega_{mn}}{[1 - (\epsilon/2) + (7/32)\epsilon^2 - (39/512)\epsilon^3]^{1/2}} \quad (22)$$

$$2\omega_{mn}[4 + \tfrac{5}{3}\epsilon^2]^{-1/2} < \sigma < 2\omega_{mn}[4 - \tfrac{1}{3}\epsilon^2]^{-1/2}$$

Other regions are very narrow and occur at

$$\sigma/2\omega_{mn} = \tfrac{1}{3}, \tfrac{1}{4}, \tfrac{1}{5}, \ldots$$

but some damping is always present and will eliminate these regions.[12] Equations (22) are in agreement with similar results given by Oniashvili[6] except for a minor disagreement in the coefficient of the ϵ^3 terms. The principal unstable region appears to be at $\frac{1}{2}$ of the exciting frequency. This tendency was detected experimentally, but a detailed quantitative correlation was not possible. In the experiment with the step loading, the mode into which the shell finally buckled had a natural frequency of 1350 cps, which is close to one-half of the ring mode frequency of 3000 cps. This tends to lend support to the results of Mathieu's equation, but it is by no means conclusive.

The solution of (21) given by Fig. 8 and by Eq. (22) implies that instability can result for *any* small value of ϵ_{mn} if σ falls in the unstable region. This paradoxical conclusion disappears when damping is included in the analysis. This is discussed by Lubkin and Stoker.[14] The work of Russian writers in this area is discussed by Beilin and Dzhanelidze,[11] who have shown that damping contracts the region of instability and shifts the higher regions to the right as shown in Fig. 12. Thus, it may be inferred that loss of dynamic stability is practically possible only for ϵ_{mn} larger than certain minimum values, which depend upon the damping and the exciting frequency.

References

[1] "Final report on buckling of shells under dynamic loads," Engineering Mechanics Lab., Space Technology Labs. Rept. 8622-0001-RU-000, EM 11-22 (October 26, 1961).

[2] Vol'mir, A. S. and Mineev, V. E., "An experimental investigation of the buckling of a shell under dynamic load," Soviet Phys.—Doklady **125**, 1002 (1959).

[3] Vol'mir, A. S., "On the stability of dynamically loaded cylindrical shells," Soviet Phys.—Doklady **123**, 806–808 (1958).

[4] Agamirov, V. L. and Vol'mir, A. S., "Behavior of cylindrical shells under dynamic loading by hydrostatic pressure or by axial compression," ARS J. **31**, 98 (1961).

[5] Markov, A. N., "Dynamic stability of anisotropic cylindrical shells," Prikl. Mat. Mekh. **13**, 145–150 (1949).

[6] Oniashvili, O. D., "Certain dynamic problems of the theory of shells," transl. by M. D. Friedman, Inc., West Newton, Mass. (Press of the Academy of Sciences of the USSR, Moscow, 1957).

[7] Lavrent'ev, M. A. and Ishlinskii, A. Yu., "Dynamic forms of loss of stability on an elastic system," Doklady Akad. Nauk SSSR **64**, 779–782 (1949); transl. by R. M. Cooper in Space Technology Labs. TR-61-5110-41. (August 1961).

[8] Kadashevich, Yu. I. and Pertsev, A. K., "On the loss of stability of a cylindrical shell under dynamic loading," Izv. AN. Otd. Tech. Nauk, Mekh. 1 Mash., no. 3, 30–33 (1960); transl. by K. N. Trirogoff and R. M. Cooper, Aerospace Corp. (June 1961).

[9] Bolotin, V. V., "Certain nonlinear problems of dynamic stability of plates," Izv. Akad. Nauk SSSR, no. 10, 47–59 (1954).

[10] Bolotin, V. V., "Behavior of thin elastic shells in response to impulsive loading," Stroit Mekhi Konstructsii, no. 2, 9–16 (1959).

[11] Beilin, E. A. and Dzhanelidze, G. Yu., "Survey of work on the dynamic stability of elastic systems," Prikl. Mat. Mekh. **16**, 635–648 (1952); transl. by K. N. Trirogoff and R. M. Cooper, Aerospace Corp. TDR-930(2119)TN-2 (November 15, 1961).

[12] Markov, A. N., "Dynamic stability of anisotropic cylindrical shells," Prikl. Mat. Mekh. **13** (1949).

[13] Yao, J. C., "Dynamic stability of cylindrical shells under static and periodic axial and radial loads," AIAA J. **1**, 1391–1396 (1963).

[14] Lubkin, S. and Stoker, J. J., "Stability of columns and strings under periodically varying forces," Quart. Appl. Math. **1**, 215–236 (1943).

[15] Donnell, L. H., "Stability of thin-walled tubes under torsion," NACA Rept. 479 (1933).

[16] Timoshenko, S. P. and Woinowsky-Krieger, S., *Theory of Plates and Shells* (McGraw-Hill Book Co. Inc., New York, 1959), 2nd ed., pp. 393–395.

[17] McLachlan, N. W., *Theory and Application of Mathieu Functions* (Oxford University Press, London, 1947), Chap. 3.

[18] Bolotin, V. V., *The Dynamic Stability of Elastic Systems* (Gostekhizdat, Moscow, 1956); transl. from the Russian by V. I. Weingarten, K. N. Trirogoff, and K. D. Gallegos, Aerospace Corp. Rept. TDR-169(3560-30)TR-Z.